Supplementary Information

Fast and continuous-flow separation of DNA-complexes and topological DNA variants in microfluidic chip format

Martina Viefhues[+], Jan Regtmeier, and Dario Anselmetti

Experimental Biophysics and Applied Nanoscience, Faculty of Physics, Bielefeld University, Universitätsstraße 25, 33615 Bielefeld, Germany

[+]corresponding author:
viefhues@physik.uni-bielefeld.de,
phone: +49-521-106-5392, fax +49-521-106-2959

Supplementary File	Title
Supplementary Results	Calculation of minimal size of DNA
Supplementary Results	Determination of polarizability
Supplementary figure 1	Fluorescence image of ridges with ROI
Supplementary figure 2	Plot of fluorescence intensity versus time
Supplementary Figure 3	Plot of $\ln \tau$ versus AC-voltage
Supplementary Results	Single experiments at bowed ridge
Supplementary Figure 4	Fluorescence intensity plots of single measurements
Supplementary Results	Characterization of DNA/RNAP-complex via AFM
Supplementary Figure 5	AFM image of DNA/RNAP stock solution
Supplementary Results	DNA experiment with 10 mM phosphate buffer
Supplementary Figure 6	DNA deflection at bowed ridge with 10 mM buffer
Supplementary Results	Calculation of radius of gyration
Supplementary Figure 7	Mean area versus time to determine diffusion constant.

Supplementary Results: Calculation of minimal size of DNA

DNA molecules are expected to be deflected if the dielectrophoretic potential is the same as for the successful separation, already presented in the miniaturized device with $W_{DEP} = -\frac{1}{2}\alpha\vec{E}^2 = 4.56 \cdot 10^{-20}\ J$. Thus, if the size/polarizability of the molecule decrease the electric field, respectively applied AC-voltage, has to increase. We calculated the minimal DNA size for the miniaturized device with 180 nm nanoslit height. The maximal applied AC-voltages were assumed to be 600 V. So DNA-fragments with polarizability of $4.4 \cdot 10^{-31}\ Fm^2$ could be deflected at the ridge. To calculate the number of base pairs N of the DNA molecule we exploit that $\alpha \propto N^v$. For exponent v different values are discussed in the literature, varying between 3 for DNA of 120 bp [38] to 0.5 for DNA of about 6.0 kbp [12]. Thus, an exact value could not be calculated but the minimal DNA size is between 3 bp and 80 bp.

Supplementary Results: Determination of polarizability

Experimentally, a defined amount of DNA is injected into the structured channel by pinched injection (see Chip Experiments). The fluorescence intensity is determined in a defined region of interest (ROI) between two ridges (Supplementary Fig.1).

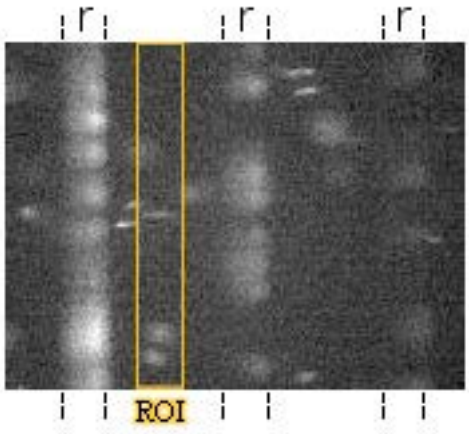

Supplementary figure 1. Fluorescence image of ridges with ROI. The fluorescent labeled DNA molecules are trapped at the ridges (r) and escape by thermal energy, statistically distributed. The mean fluorescence intensity is determined in the ROI.

The fluorescence intensity within the ROI is plotted versus time and fitted with a gaussian function. In Supplementary Fig.2 the graph of fluorescence is depicted for instance.

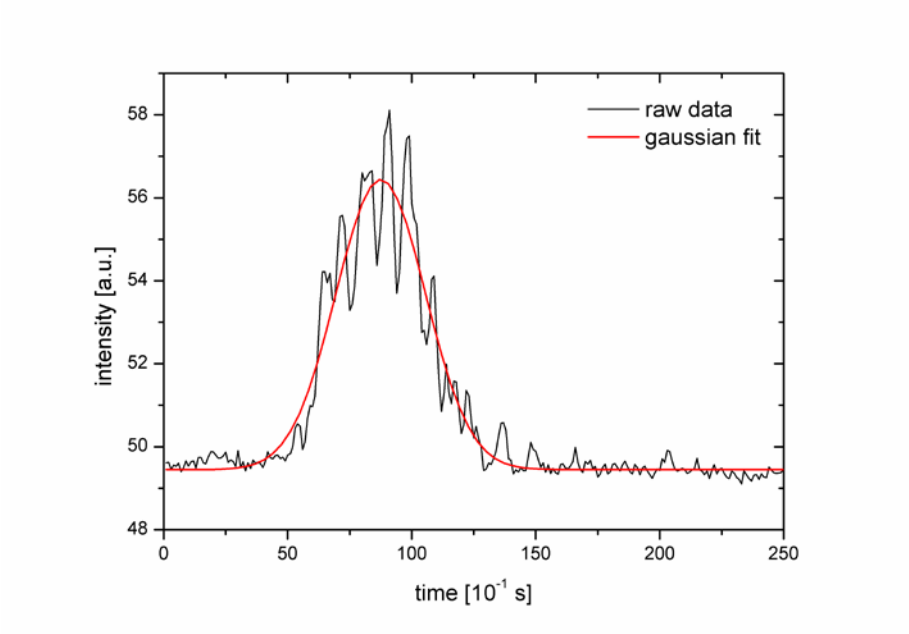

Supplementary figure 2. Plot of fluorescence intensity versus time. The mean fluorescence intensity within the ROI is plotted versus time and fitted with a Gaussian function.

This procedure was performed for varying U_{AC}. The polarizability of DNA and DNA-complexes was determined by plotting the escape times τ for different applied AC-voltages and fitted with $\ln \tau = const + c\frac{\alpha U_{AC}^2}{kT}$ (see also Theory). In Supplementary Fig. 3 the graph for the 6 kbp DNA is depicted for instance.

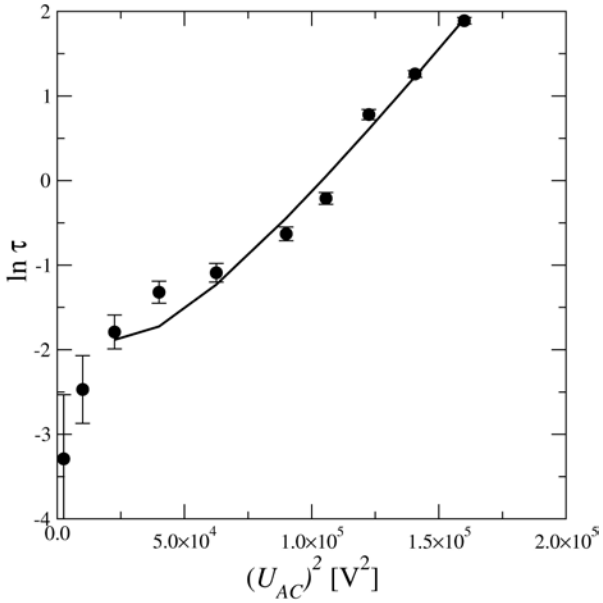

Supplementary figure 3. Plot of $\ln \tau$ versus AC-voltage. Escape times τ for different applied AC voltages. The linear fit with logarithmic corrections is used for calculating polarizabilities (see Theory).

Supplementary Results: Single experiments at bowed ridge

During the separation experiments two peaks were observed downstream of the ridge (see Results). To identify the species, experiments with single species were performed under identical conditions (see Supplementary Fig.4 for instance). As expected the larger 6.0 kbp DNA was deflected, whereas the smaller 2.686 kbp DNA was not affected. For separation of DNA-complexes the complex was deflected, whereas the pure DNA was not affected.

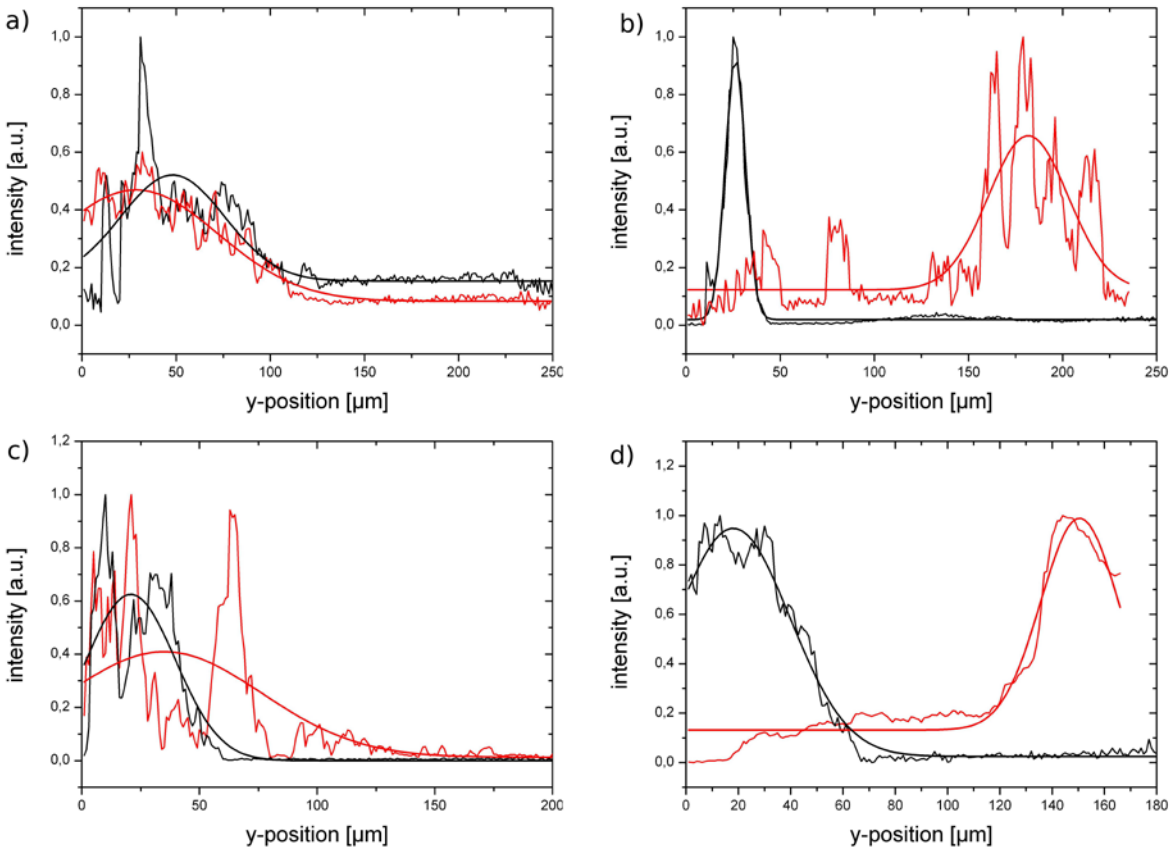

Supplementary figure 4. Fluorescence intensity plots of single measurements. Same conditions as separation experiment (black: fluorescence intensity upstream, red: fluorescence intensity downstream). a) and b) 2.686 kbp DNA and 6.0 kbp DNA at identical conditions. The 2.686 kbp DNA was not deflected, whereas the 6.0 kbp DNA was fully deflected at the ridge. c) and d) 6.0 kbp DNA and DNA actinomycin D complex. The pure DNA was not deflected, whereas the DNA complex was fully deflected at the ridge.

Supplementary Results: Characterization of DNA/RNAP-complex via AFM
For visualization of *E.coli* RNA polymerase (RNAP) core enzyme binding to DNA, AFM (BioScope, Veeco, USA) images were taken. Stock solution of DNA/RNAP-complexes was diluted to 373 pM (20 fold) in 1 mM phosphatebuffer (1 mM EDTA and 2 mM Trolox) and 1.5 µl thereof put on a APTES ((3-aminopropyl)trietoxysilane, Sigma Aldrich, Germany) silanized mica, dried, and rinsed with deionized water to remove salt crystals. The cantilever (Tap 300-AL, Budget Sensors, BG) was operated in tapping mode (excitation frequency 300 kHz).
In Supplementary Fig.5 a topography image of the DNA/RNAP-complex solution is depicted. The white dots are *Escherichia coli* RNA core polymerase and the white lines are DNA strands. An inhomogeneous distribution of polymerase along the DNA strand can be seen. Rivetti et al. find some DNA strands with more than one polymerase and some DNA strands with no polymerase, either [48]

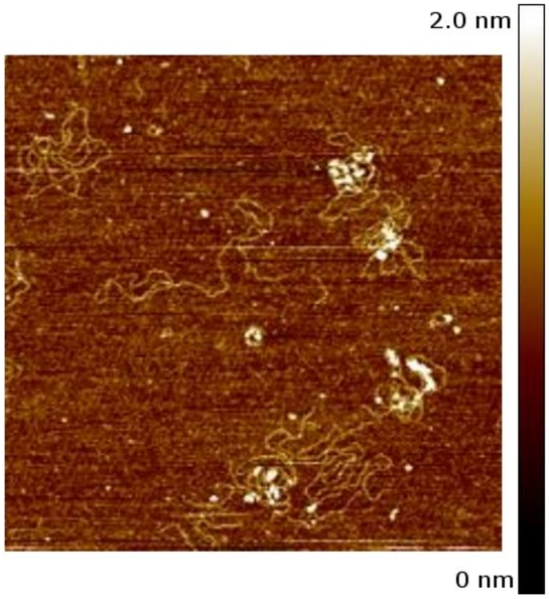

Supplementary figure5. AFM image of DNA/RNAP stock solution. AFM image (topography) of 6.0 kbp DNA/RNAP-complex solution before performance of separation. The proteins (bright spots on DNA strands) are not homogeneously distributed along the DNA strand (*cf.* [48]).

Supplementary Results: DNA experiment with 10 mM phosphate buffer

Since all experiments were performed in 1 mM phosphate buffer to reduce joule heating effects [16] we run the device for 10 mM phosphate buffer, too (see supplementary Fig.6). Therefore, 6.0 kbp DNA was injected and fully deflected at the ridge demonstrating the ability to use buffer with higher ionic strength, either.

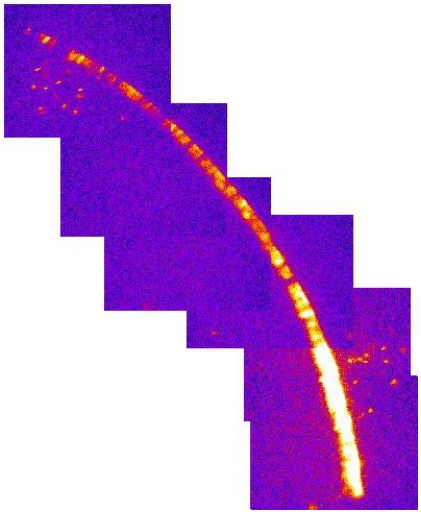

Supplementary figure 6. DNA deflection at bowed ridge with 10 mM buffer. Direction of flow is from left to right. 6.0 kbp DNA is trapped and deflected at the ridge for 10 mM phosphate solution (U_{AC} = 650 V, ω =350 Hz).

Supplementary Results: Calculation of radius of gyration

The radius of gyration could be changed by intercalation or alignment of antibiotic and polymerase at DNA [46,47,49,50]. To check the influence of the DNA-complexes to the radius of gyration diffusion experiments were performed, when the hydrodynamic radius r_h can be determined by the diffusion constant D by $D = \frac{kT}{6\pi\eta r_h}$, with k Boltzmann constant, T temperature and η viscosity of the medium [51]. By plotting $< R^2 >$ versus time the diffusion constant can be determined by the slope (see Supplementary Fig.7) with $D = \frac{< R^2 >}{4t}$, with mean area $< R^2 >$ and time t . The radius of gyration r_g is related to the hydrodynamic radius via $r_g = 1.51 \cdot r_h$ [52]. The Diffusion constant, and so the radius of gyration, differs only slightly within the experimental error for the 6.0 kbp DNA and DNA-complexes, whereas for the 2.686 kbp DNA the diffusion constant is significantly greater.

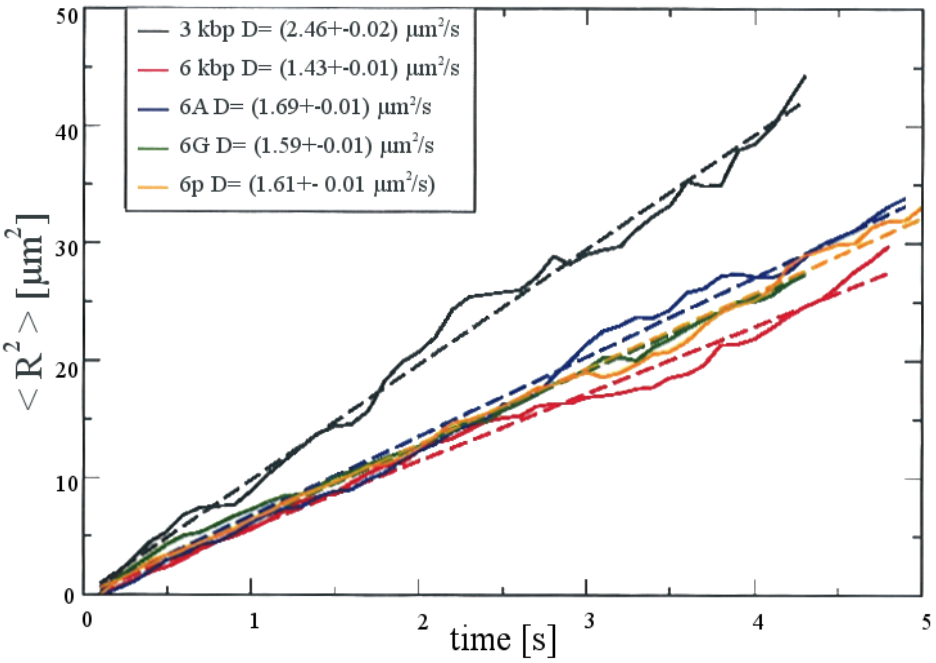

Supplementary figure 7. Mean area versus time to determine diffusion constant D. Abbreviations: 3 kbp stands for 2.686 kbp DNA, 6A is actinomycin D DNA complex, 6G stands for diffusion experiment of 6.0 kbp DNA with glycerine, 6p is polymerase DNA complex.

Additional References:

[48] Rivetti, C., Guthold, M., and Bustamante, C. *EMBO J* **18**(16), 4464–4475 Aug (1999).
[49] Stonington, O. G. and Pettijohn, D. E. *Proc Natl Acad Sci U S A* **68**(1), 6–9 Jan (1971).
[50] Yaneva, J., Paneva, E., Zacharieva, S., Yossifova, L., and Zlatanova, J. *Biotechnology & Biotechnological Equipment* **23**, 1048–1052 (2009).
[51] Einstein, A. *Ann. Phys.* **17**, 549–560 (1905).
[52] Doi, M. and Edwards, S. *The theory of polymer dynamics*. Clarendon Press, Oxford, (1986).